Phorbasins G–K: new cytotoxic diterpenes from a southern Australian marine sponge, *Phorbas* sp.†

Hua Zhang, Jodie M. Major, Richard J. Lewis and Robert J. Capon*

Received 27th May 2008, Accepted 21st July 2008
First published as an Advance Article on the web 28th August 2008
DOI: 10.1039/b808866g

Fractionation of a cytotoxic extract obtained from a southern Australian marine sponge, *Phorbas* sp., yielded the known diterpenes phorbasins B–F (**1–5**) together with five new members of the phorbasin family, phorbasins G–K (**6–10**). Structures were assigned to the new phorbasins based on detailed spectroscopic analysis. A preliminary structure activity relationship (SAR) evaluation based on the co-metabolites phorbasins B–K (**1–10**) revealed aspects of the phorbasin pharmacophore.

Introduction

During an earlier chemical investigation of a cytotoxic extract obtained from a *Phorbas* sp., collected during scientific trawling operations in the Great Australian Bight, Capon and Zhang reported the re-isolation and structure revision of two known diterpenes, phorbasins B–C (**1–2**), along with the discovery and structure elucidation of a selection of unprecedented diterpenyl taurines, phorbasins D–F (**3–5**).[1] In an extension to that earlier study we have continued and completed investigations into this *Phorbas* sp., and report a further five new members of the phorbasin structure class, phorbasins G–K (**6–10**), of which phorbasins I and J (**8–9**) are likely solvolysis artifacts. We also report a comparative assessment of phorbasin cytotoxicity, employing all available members of the phorbasin structure class.

Results and discussion

An earlier chemical investigation of the EtOH extract of a Great Australian Bight *Phorbas* sp. yielded five *Phorbas* diterpenes, identified as the known phorbasins B–C (**1–2**) and the new unprecedented terpenyl-taurines phorbasins D–F (**3–5**).[1] Also detected during those earlier studies were a selection of minor, more cytotoxic phorbasin co-metabolites. This report describes the isolation and identification of the principle cytotoxic agents in the *Phorbas* extract as the new phorbasin analogues, phorbasins G–K (**6–10**). Phorbasins G–K (**6–10**) were isolated by the use of solvent partitioning, reverse phase SPE (solid phase extraction) and HPLC and their structures assigned by detailed spectroscopic analysis as detailed below.

High resolution ESI(+)MS analysis of phorbasin G (**6**) revealed a *pseudo* molecular ion (M + Na) consistent with a molecular formula ($C_{20}H_{30}O_3$, Δmmu −0.2) incorporating six double bond equivalents (DBE) and suggestive of a deoxy analogue of phorbasin B (**1**). Analysis of the NMR ($CDCl_3$) data for **6** (Tables 1 and 2) confirmed this hypothesis, with diagnostic resonances for the 17-oxymethylene in **1** (δ_H 4.23 (br d, 15.0 Hz), 4.28 (br d, 15.0 Hz); δ_C 59.7)[1] replaced in **6** by an allylic methyl (δ_H 1.89 (s); δ_C 15.7). Excellent comparisons between the remaining NMR data for **1** and **6** supported the assignment of common structural features between these co-metabolites. As with **1**, analysis of the NMR ($CDCl_3$) data for **6** revealed measurements for $J_{9,10}$ (15.1 Hz) and $J_{12,13}$ (15.4 Hz), and a shielded C-18 (δ_C 17.1), consistent with *E* configurations about $\Delta^{9,10}$, $\Delta^{12,13}$ and $\Delta^{7,8}$ respectively, while measurements for $J_{1,6}$ (3.2 Hz) and $J_{5,6}$ (12.2 Hz) defined the relative configuration about the cyclohexenone moiety as shown. Thus **6** was identified as the 17-deoxy analogue of the co-metabolite **1**, and on biogenetic grounds was assigned a common absolute stereochemistry.

High resolution ESI(+)MS analysis of phorbasin H (**7**) revealed a *pseudo* molecular ion (M + Na) consistent with a molecular formula ($C_{22}H_{32}O_4$, Δmmu 0.9) incorporating seven DBE and suggestive of an acetoxy analogue of phorbasin G (**6**). Analysis of the NMR (C_6D_6) data for **7** (Tables 1 and 2) confirmed this hypothesis, with diagnostic resonances for an acetoxy moiety (δ_H 1.59 (s); δ_C 169.6, 20.6) together with characteristic deshielding of the H-1 oxymethine (δ_H 5.29) compared to **6** (δ_H 4.34). Excellent comparisons between the NMR data for **7** and **6**, including key H–H coupling constants, were supportive of common structural features between these co-metabolites, including configurations about all chiral centres and double bonds. Thus **7** was identified as the C-1 acetate of the co-metabolite **6**, and on biogenetic grounds was assigned a common absolute stereochemistry.

High resolution ESI(+)MS analysis of phorbasin I (**8**) revealed a *pseudo* molecular ion (M + Na) consistent with a molecular formula ($C_{24}H_{36}O_5$, Δmmu 1.1) incorporating seven DBE and suggestive of an ethoxy analogue of phorbasin H (**7**). Analysis of the NMR (C_6D_6) data for **8** (Tables 1 and 2) confirmed this hypothesis, with diagnostic resonances for an ethoxy moiety (δ_H 1.03 (t, 7.0 Hz), 3.23 (q, 7.0 Hz); δ_C 15.6, 67.1) whose regiochemistry was determined by HMBC correlations from OCH_2CH_3 to C-17. Excellent comparisons between the NMR (C_6D_6) data for **8** and **7** were supportive of common configurations about all chiral centres and double bonds. Thus **8** was identified as a C-17 ethoxy analogue of the co-metabolite **7**, and on biogenetic grounds was assigned a common absolute stereochemistry. The appearance of an ethoxy moiety in **8** was strongly suggestive of

Institute for Molecular Bioscience, The University of Queensland, St Lucia, Queensland, 4072, Australia. E-mail: r.capon@imb.uq.edu.au; Fax: 617 3346 2090; Tel: 617 3346 2979

† Electronic supplementary information (ESI) available: Bioassay data for crude extracts, together with tabulated 1D and 2D NMR data and ^{1}H NMR spectra for new compounds, and cytotoxicity curves for all compounds. See DOI: 10.1039/b808866g

Table 1 ^{1}H NMR (600 MHz) data for phorbasins G–K (**6–10**)

No	**6**[a]	**7**[b]	**8**[b]	**9**[b]	**10**[c]
1	4.34 (dd, 5.7, 3.2)	5.29 (dd, 5.7, 3.7))	5.46 (dd, 5.7, 3.7)	5.50 (dd 3.6, 2.9)	4.14 (m)
2	6.76 (dd, 5.7, 1.3)	6.22 (dd, 5.7, 1.4)	6.92 (d, 5.7)	4.11 (dd, 3.6, 3.6)	5.82 (m)
3				2.94 (m)	
4					3.98 (br d, 7.8)
5	4.65 (d, 12.2)	4.51 (d, 12.2)	4.56 (d, 12.2)	4.33 (d, 11.7)	3.93 (dd, 11.8, 7.8)
6	2.62 (dd, 12.2, 3.2)	2.41 (dd, 12.2, 3.7)	2.44 (dd, 12.2, 3.7)	2.95 (m)	2.25 (dd, 11.8, 3.9)
8	6.15 (br d, 10.7)	6.10 (br d, 10.7)	6.09 (br d, 10.7)	6.20 (br d, 10.7)	5.95 (br d, 10.8)
9	6.30 (dd, 15.1, 10.7)	6.44 (dd, 15.1, 10.7)	6.43 (dd, 15.1, 10.7)	6.44 (dd, 15.1, 10.7)	6.35 (ddd, 15.1, 10.8, 1.2)
10	5.71 (dd, 15.1, 6.9)	5.70 (dd, 15.1, 6.9)	5.69 (dd, 15.1, 6.9)	5.67 (dd, 15.1, 6.9)	5.56 (dd, 15.1, 6.9)
11	2.90 (m)	2.90 (m)	2.89 (m)	2.88 (m)	2.88 (m)
12	5.33 (dd, 15.4, 6.5)	5.43 (m)	5.42 (m)	5.40 (m)	5.36 (dd, 15.3, 6.0
13	5.38 (dt, 15.4, 6.8)	5.43 (m)	5.42 (m)	5.42 (m)	5.39 (dt, 15.3, 6.1)
14	1.87 (dd, 6.8, 6.8)	1.90 (dd, 6.2, 6.2)	1.89 (dd, 6.2, 6.2)	1.89 (dd, 6.1, 6.1)	1.89 (dd, 6.1, 6.1)
15	1.58 (m)	1.55 (m)	1.54 (m)	1.55 (m)	1.59 (m)
16/20	0.86 (d, 6.6)	0.88 (d, 6.7)	0.88 (d, 6.7)	0.88 (d, 6.7)	0.89 (d, 6.7)
17	1.89 (s)	1.61 (s)	4.13 (br d, 14.6)	3.92 (dd, 9.3, 4.9)	4.21 (br d, 14.1)
			4.05 (dd, 14.6, 1.6)	3.82 (dd, 9.3, 9.3)	4.16 (br d, 14.1)
18	1.90 (s)	1.88 (s)	1.87 (s)	1.87 (s)	1.91 (s)
19	1.09 (d, 6.9)	1.11 (d, 6.9)	1.10 (d, 6.9)	1.10 (d, 6.9)	1.09 (d, 6.9)
CH_3CO		1.59 (s)	1.55 (s)	1.56 (s)	
5-OH		3.62 (br s)	3.55 (br s)		
C-2 OCH_2CH$_3$				3.41 (m)	
				3.27 (m)	
C-2 OCH$_2$CH_3				0.93 (t, 7.0)	
C-17 OCH_2CH$_3$			3.23 (q, 7.0)	3.34 (m)	
				3.27 (m)	
C-17 OCH$_2$CH_3			1.03 (t, 7.0)	1.04 (t, 7.0)	

[a] In $CDCl_3$. [b] In C_6D_6. [c] In CD_3OD.

solvolysis during prolonged storage of the *Phorbas* specimen in EtOH. A plausible mechanism for formation of **8** could involve the nucleophilic displacement by EtOH of a suitable C-17 leaving group in a co-metabolite precursor, such as the taurine residue in phorbasin D (**3**).

Table 2 ^{13}C NMR data for phorbasins G–K (**6–10**)

No	**6***[a]	**7**#[b]	**8**#[b]	**9***[b]	**10***[c]
1	65.4	69.3	68.8	71.7	70.2
2	142.5	139.5	139.1	78.4	125.2
3	135.3	136.5	137.6	49.2	143.2
4	201.2	201.0	200.2	209.1	76.2
5	69.9	71.0	71.0	73.3	71.6
6	55.1	53.9	53.8	53.7	55.4
7	131.5	132.8	132.6	132.6	136.4
8	129.6	130.0	130.0	129.2	129.9
9	124.1	125.4	125.4	125.6	126.4
10	140.6	139.4	139.5	139.1	138.5
11	40.1	40.6	40.6	40.6	41.2
12	135.2	136.1	136.1	136.2	137.1
13	128.5	128.7	128.6	128.7	129.0
14	42.2	42.7	42.7	42.7	43.3
15	28.6	29.1	29.1	29.1	29.8
16/20	22.5	22.8	22.8	22.8	22.8
17	15.7	15.7	66.9	65.5	63.2
18	17.1	16.4	16.5	16.7	16.6
19	20.8	21.2	21.2	21.2	21.3
*C*H$_3$CO		20.6	20.6	20.7	
CH$_3$*C*O		169.6	169.5	169.5	
C-2 O*C*H$_2$CH$_3$				66.9	
C-2 OCH$_2$*C*H$_3$				15.8	
C-17 O*C*H$_2$CH$_3$			67.1	67.1	
C-17 OCH$_2$*C*H$_3$			15.6	15.7	

*Recorded at 600 MHz, #measured at 400 MHz.[a] In $CDCl_3$. [b] In C_6D_6. [c] In CD_3OD. All assignments supported by gHSQC and HMBC analysis.

High resolution ESI(+)MS analysis of phorbasin J (**9**) revealed a *pseudo* molecular ion (M + Na) consistent with a molecular formula ($C_{26}H_{42}O_6$, Δmmu −0.2) incorporating six DBE and suggestive of an EtOH addition adduct to phorbasin I (**8**). Supportive of this hypothesis, the NMR (C_6D_6) data for **9** (Tables 1 and 2) revealed resonances consistent with reduction of $\Delta^{2,3}$ to yield (a) diastereotopic H_2-17 methylene resonances (δ_H 3.92 and 3.82) with coupling to H-3 (δ_H 2.94) ($J_{3,17a}$ 4.9 Hz, $J_{3,17b}$ 9.3 Hz), (b) an ethoxy methylene (OCH_2CH$_3$, δ_H 3.34 and 3.27) with HMBC correlations to C-17 (δ_C 65.5), (c) replacement of the H-2 olefinic methine resonance common to phorbasins B–I (**1–8**) with an oxymethine resonance (δ_H 4.11 (dd, 3.6, 3.6 Hz); δ_C 78.4) displaying COSY correlations to H-1 (δ_H 5.50) and H-3, and (d) a second diastereotopic ethoxy methylene (OCH_2CH$_3$, δ_H 3.41 and 3.27) with HMBC correlations to C-2. These observations were consistent with addition of EtOH across $\Delta^{2,3}$ as indicated. Excellent comparisons between the NMR (C_6D_6) data for the C-6 side chain in **9** and **8** supported common structural features including configurations about all double bonds. Relative configuration about the cyclohexanone moiety in **9** was assigned by consideration of ^{1}H NMR (C_6D_6) coupling constants and ROESY correlations. The magnitude of $J_{5,6}$ (11.7 Hz) required an H-5 to H-6 *pseudo* diaxial relationship, while a ROESY correlation between H-5 and H-3 dictated a *pseudo* diaxial relationship. Similarly, values for $J_{2,3}$ (3.6 Hz) and $J_{1,6}$ (2.9 Hz) required that H-2 and H-1 adopt *pseudo* equatorial configurations. Thus **9** can be assigned the structure as shown, and on biogenetic grounds can be assigned an absolute stereochemistry common with all other

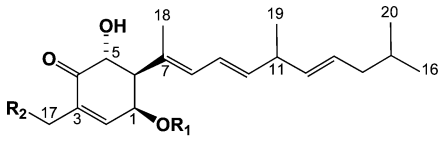

	R_1	R_2
phorbasin B (1)	H	OH
phorbasin C (2)	Ac	OH
phorbasin D (3)	H	$NHCH_2CH_2SO_3H$
phorbasin G (6)	H	H
phorbasin H (7)	Ac	H
phorbasin I (8)	Ac	OEt

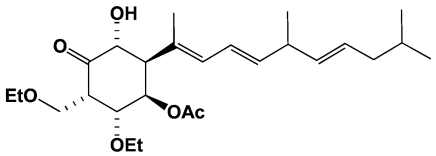

phorbasin J (9)

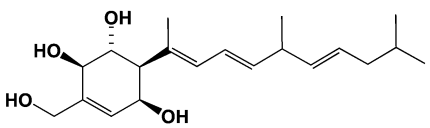

phorbasin K (10)

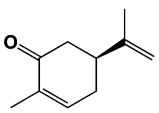

(S)-carvone (11)

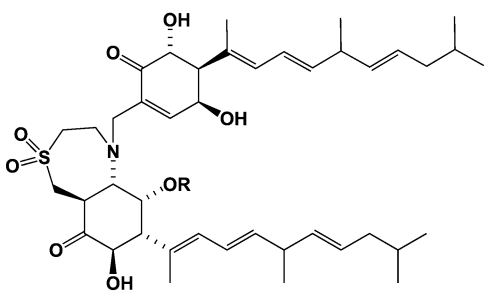

phorbasin E (4) R = H
phorbasin F (5) R = Ac

phorbasins. As with **8**, the appearance of ethoxy residues in **9** was strongly suggestive of solvolysis during long term storage in EtOH. We propose that **9** is likely formed by Michael addition of EtOH to C-2 on the co-metabolite/solvolysis artifact **8**, with α facial stereocontrol resulting from the steric influence of the C-1 acetoxy functionality. Quenching of the resulting enolate could proceed by β facial protonation at C-3, thereby establishing the relative stereochemistry about the cyclohexanone moiety as shown.

High resolution ESI(+)MS analysis of phorbasin K (**10**) revealed a *pseudo* molecular ion (M + Na) consistent with a molecular formula ($C_{20}H_{32}O_4$, Δmmu 1.0) incorporating five DBE and suggestive of a dihydro analogue of phorbasin B (**1**). Supportive of this hypothesis the NMR (CD_3OD) data for **10** (Tables 1 and 2) revealed an absence of the ketone carbonyl resonance (δ_C ~ 201) characteristic of phorbasins B–I (**1–8**), and the appearance of an H-4 oxymethine (δ_H 3.98) coupled to H-5 ($J_{4,5}$ 7.8 Hz). Excellent comparisons between the NMR data for the C-6 side chain in **10** and **1** supported common structural features including configurations about all double bonds. Likewise, consideration of $J_{1,6}$ (3.9 Hz) and $J_{5,6}$ (11.8 Hz) permitted assignment of a relative configuration about C-1, C-5 and C-6 common with that previously assigned to **1**, while the magnitude of $J_{4,5}$ (7.8 Hz) was suggestive of a *pseudo* equatorial C-4 hydroxy moiety. Paucity of material precluded a 2D NMR ROESY approach to assignment of relative configuration. Thus **10** can be assigned the structure as shown, and on biogenetic grounds can be assigned an absolute stereochemistry common with all other phorbasins.

While we have attributed absolute stereochemistry to phorbasins G–K (**6–10**) on biogenetic grounds,[1] consideration of the CD data provides an independent means to validate this assignment for phorbasins G–I (**6–8**). Phorbasins G–I (**6–8**) possess a common cyclohexenone moiety and display comparable n–π* Cotton effects (330 (+0.7), 330 (+0.9) and 337 (+0.7) nm respectively) to phorbasins B–F (**1–5**),[1] indicative of a common 1*S*,5*R*,6*S* absolute configuration. The stereochemistry about C-11 in all the phorbasins remains undetermined.

The *in vitro* cytotoxicity data for phorbasins B–K (**1–10**) against both normal (NFF) and human cancer (A549, HT29 and MM96L) cell lines are shown in Table 3. Analysis of this data revealed a prevailing structure activity relationship correlating with the presence of an α,β-unsaturated ketone functionality. For example, whereas modest GI_{50} potency (~1–8 μM) and selectivity for cancer *versus* NFF cell lines (~1 to 9 fold) were apparent for phorbasins B–I (**1–8**), LC_{50} measurements highlight phorbasins B (**1**), C (**2**), G (**6**), H (**7**) and I (**8**) as retaining substantial potency and selectivity. Of note, all these latter compounds possess a common unhindered cyclohex-2-enone functionality. By contrast, phorbasins J (**9**) and K (**10**), both of which lack a cyclohex-2-enone functionality, are the least selectively cytotoxic of the phorbasins investigated. This preliminary structure activity relationship data, based on the cytotoxic properties of co-metabolites, is suggestive of a Michael acceptor mechanism-of-action. Indicative of the potential of some phorbasins to engage in Michael additions are the solvolysis analogues phorbasins I (**8**) and J (**9**), and the dimers phorbasins E (**4**) and F (**5**).

To test the hypothesis that the phorbasin pharmacophore is merely a Michael acceptor embedded within a new carbon skeleton, we screened the commercially available monoterpene *S*-(+)-carvone (**11**). The natural product **11** incorporates a cyclohex-2-enone moiety very similar to that found in the phorbasins, and is well known to be chemically reactive as a Michael acceptor. That said, when tested across 0.2 to 70 μM in 10-fold increments, **11** failed to produce any significant cytotoxicity on A549, HT29, MM96L and NFF cell lines in three separate experiments (Table 3), indicating that the potential for Michael addition alone is

Table 3 Cell cytotoxicity data (μM) for phorbasins B–K (**1–10**)[a]

#		NFF	A549	HT29	MM96L
1	GI_{50}	6.0	3.0	3.0	3.0
	TGI_{50}	13.5	4.5	4.5	4.5
	LC_{50}	26.9	6.0	6.0	6.0
2	GI_{50}	5.3	2.7	2.7	2.7
	TGI_{50}	12.0	4.0	4.0	4.0
	LC_{50}	23.9	6.6	6.6	6.6
3	GI_{50}	15.9	3.4	7.9	4.5
	TGI_{50}	>22.7	9.6	>22.7	10.2
	LC_{50}	>22.7	~22.7	>22.7	15.9
4	GI_{50}	7.4	2.7	4.7	2.0
	TGI_{50}	~13.5	5.4	6.7	4.7
	LC_{50}	>13.5	9.4	9.4	8.1
5	GI_{50}	6.4	4.5	4.5	2.2
	TGI_{50}	10.9	6.4	6.4	5.1
	LC_{50}	>12.8	10.2	10.2	8.0
6	GI_{50}	9.4	4.7	3.1	3.1
	TGI_{50}	22.0	12.6	4.7	4.7
	LC_{50}	~ 31.4	18.9	7.9	7.1
7	GI_{50}	7.6	2.8	2.8	0.8
	TGI_{50}	15.3	9.7	4.2	5.6
	LC_{50}	~ 27.8	16.7	5.6	13.9
8	GI_{50}	6.2	2.5	2.5	1.7
	TGI_{50}	13.6	3.7	3.7	3.7
	LC_{50}	~ 24.8	5.6	5.6	5.6
9	GI_{50}	8.9	3.9	6.1	2.2
	TGI_{50}	22.2	8.9	10.0	8.9
	LC_{50}	>22.2	15.6	16.7	15.6
10	GI_{50}	>29.8	11.9	>29.8	6.0
	TGI_{50}	>29.8	>29.8	>29.8	>29.8
	LC_{50}	>29.8	>29.8	>29.8	>29.8
11	GI_{50}	>70	>70	>70	>70
	TGI_{50}	>70	>70	>70	>70
	LC_{50}	>70	>70	>70	>70

[a] NFF—neonatal foreskin fibroblast; A549-carcinoma (lung); HT29-colorectal adenocarcinoma (colon); MM96L—malignant melanoma (skin). GI_{50}, concentration required for 50% inhibition of growth; TGI, concentration required for total inhibition of growth; and LC_{50}, concentration required to kill 50% of cells available at commencement of the assay. Averaged values within ±10% for all cancer cell lines or within ±20% for the NFF cell line.

insufficient to explain the phorbasin cytotoxicity data. In the case of the phorbasins we speculate that added structural complexity in the form of hydroxylation and an extended lipophilic side chain influence polarity (H-donors/acceptors) and solubility (cLogP) and very likely play a significant role in defining the cytotoxic pharmacophore. Such hypotheses are best assessed by future synthetic investigations.

Experimental section

General experimental procedures

As previously reported.[1]

Animal material

As previously reported.[1]

Extraction and isolation

The extraction, partition and SPE fractionation of the crude extracts, along with the isolation procedures of phorbasins B–F (**1–5**) are as previously reported.[1]

HPLC analysis revealed similar chemical compositions for the first and second C_{18} SPE fractions, which were combined and further separated by C_8 HPLC (4.0 mL min^{-1} 15 min gradient elution from 60% to 30% H_2O–MeCN followed by a 3 min hold) to yield in order of elution phorbasin K (**10**) (0.5 mg, 0.09%) and phorbasin G (**6**) (2.2 mg, 0.62%). The third C_{18} SPE fraction was purified by C_8 HPLC (4.0 mL min^{-1} 15 min gradient elution from 35% to 20% H_2O–MeCN followed by a 3 min hold) to yield in order of elution phorbasin G (**6**) (1.4 mg, 0.62%), phorbasin H (**7**) (2.0 mg, 0.34%), phorbasin I (**8**) (1.4 mg, 0.24%) and phorbasin J (**9**) (1.5 mg, 0.26%). All yields are calculated as a weight to weight estimate against total yield from the crude 1.17 g extract.

Bioassay

Cell culture and reagents

A549 (human lung carcinoma; ATCC CCL-185); HT29 (human colorectal adenocarcinoma; ATCC HTB-38); SkMel28 (human melanoma; ATCC HTB-72); DU145 (human prostate carcinoma; ATCC HTB-81) were obtained from the American Type Culture Collection. The human melanoma cell line MM96L,[2] and the human ovarian cancer cell lines CI80_13s and JAM[3] have been described previously. Normal dermal fibroblasts were isolated from neonatal foreskins. All cells were cultured in RPMI 1640 (Gibco, Invitrogen, Carlsbad, CA) supplemented with 10% FBS (Gibco, Invitrogen, Carlsbad, CA) at 37 °C, 5% CO_2 and 99% humidity. Routine mycoplasma tests were performed and were negative throughout these studies.

In vitro cytotoxicity assay

Cells were seeded (5 000 per well) into individual 96-well tissue culture plates (NUNC, Rochester, NY) and grown for 24 h before treatment. Test compounds or mixtures were dissolved in 100% MeOH and diluted in complete medium. The MeOH concentration in the medium was kept to <1%. Controls (1% MeOH treatment) and test treatments were performed in triplicate, and each experiment in duplicate. Three days after treatment initiation, cells were washed with phosphate-buffered saline (PBS), fixed with methylated spirits, and total protein was determined using sulforhodamine B (SRB)[4] as described previously. Briefly, at the end of the required treatment time, medium was removed from the plates, and cells were washed twice with PBS. Cells were then fixed with methylated spirits for a minimum of 15 min. After this time the cells were washed with water twice and stained with 50 μL per well of sulforhodamine B (SRB) solution (0.4% SRB (w/v) in 1% (v/v) acetic acid) for at least 30 min. The SRB solution was removed from the wells and plates rapidly washed twice with 1% (v/v) acetic acid. Protein bound dye was then solubilised by addition of 100 μL of 10 mM unbuffered Tris and incubated at room temperature for 15 min. Plates were read at 564 nm on the EnVision 2102 multilabel reader (PerkinElmer, Wallace, Oy). Data was presented as a percentage of control cell protein and analysed using Excel (Microsoft).

Growth inhibition of 50% (GI_{50}) was calculated from $[(Ti - Tz)/(C - Tz)] \times 100 = 50$, total growth inhibition (TGI) from $Ti = Tz$ and lethal concentration of 50% (LC_{50}) from $[(Ti - Tz)/Tz] \times 100 = -50$, where Ti = test growth, Tz = time zero, and C = control

growth. When cytotoxicity for any parameter is not reached, the value is expressed as a greater than the maximum concentration tested.

Phorbasin G (6). White solid; $[\alpha]_D^{22}$ –86.7 (*c* 0.18, MeOH); UV (MeOH) λ_{max} (log ε) 238 (4.22) nm; CD (MeOH) λ ($\Delta\varepsilon$) 330 (+0.7), 231 (–4.1) nm; ^{1}H NMR Table 1; ^{13}C NMR Table 2; ESIMS *m/z* (positive) 319.1 $[M + H]^+$, 341.2 $[M + Na]^+$, 659.3 $[2M + Na]^+$; HRESIMS *m/z* 341.2089 (calculated for $C_{20}H_{30}NaO_3$, 341.2087).

Phorbasin H (7). White solid; $[\alpha]_D^{22}$ –164.0 (*c* 0.10, MeOH); UV (MeOH) λ_{max} (log ε) 237 (4.38) nm; CD (MeOH) λ ($\Delta\varepsilon$) 330 (+0.9), 237 (–16.6) nm; ^{1}H NMR ($CDCl_3$, 400 MHz) δ_H 6.71 (br d, $J = 5.9$ Hz, H-2), 6.23 (dd, $J = 15.1$, 10.7 Hz, H-9), 6.01 (br d, $J = 10.7$ Hz, H-8), 5.61 (dd, $J = 10.7$, 6.7 Hz, H-10), 5.47 (dd, $J = 5.9$, 3.7 Hz, H-1), 5.34 (m, H-13), 5.33 (m, H-12), 4.66 (d, $J =$ 12.2 Hz, H-5), 3.53 (br s, 5-OH), 2.87 (m, H-11), 2.73 (dd, $J =$ 12.2, 3.7 Hz, H-6), 2.0 (3H, s, *Me*CO), 1.88 (3H, s, H-18), 1.86 (3H, s, H-17), 1.85 (2H, overlapping, H-14), 1.56 (m, H-15), 1.07 (3H, d, $J = 6.9$ Hz, H-19), 0.85 (6H, d, $J = 6.7$ Hz, H-16/20), and Table 1; ^{13}C NMR Table 2; ESIMS *m/z* (positive) 383.2 $[M +$ $Na]^+$, 743.4 $[2M + Na]^+$; HRESIMS *m/z* 383.2184 (calculated for $C_{22}H_{32}NaO_4$, 383.2193).

Phorbasin I (8). White solid; $[\alpha]_D^{22}$ –81.3 (*c* 0.14, MeOH); UV (MeOH) λ_{max} (log ε) 238 (4.26) nm; CD (MeOH) λ ($\Delta\varepsilon$) 337 (+0.7), 237 (–8.4) nm; ^{1}H NMR Table 1; ^{13}C NMR Table 2; ESIMS *m/z* (positive) 427.2 $[M + Na]^+$, 831.5 $[2M + Na]^+$; HRESIMS *m/z* 427.2444 (calculated for $C_{24}H_{36}NaO_5$, 427.2455).

Phorbasin J (9). White solid; $[\alpha]_D^{22}$ –25.4 (*c* 0.15, MeOH); UV (MeOH) λ_{max} (log ε) 243 (4.16) nm; CD (MeOH) λ ($\Delta\varepsilon$) 285 (+1.7), 246 (–4.1) nm; ^{1}H NMR Table 1; ^{13}C NMR Table 2; ESIMS *m/z* (positive) 473.3 $[M + Na]^+$, 923.5 $[2M + Na]^+$; HRESIMS *m/z* 473.2876 (calculated for $C_{26}H_{42}NaO_6$, 473.2874).

Phorbasin K (10). Colorless gum; $[\alpha]_D^{22}$ –41.9 (*c* 0.05, MeOH); UV (MeOH) λ_{max} (log ε) 242 (4.16) nm; CD (MeOH) λ ($\Delta\varepsilon$) 242 (–1.7), 212 (+1.3) nm; ^{1}H NMR Table 1; ^{13}C NMR Table 2; ESIMS *m/z* (positive) 359.2 $[M + Na]^+$, 695.3 $[2M + Na]^+$, (negative) 381.2 $[M + HCO_2]^-$; HRESIMS *m/z* 359.2183 (calculated for $C_{20}H_{32}NaO_4$, 359.2193).

Acknowledgements

The authors would like to thank L. Goudie for sponge taxonomy, C. Cuevas (PharmaMar) for *in vitro* anticancer screening, and G. MacFarlane (The University of Queensland) for the acquisition of HRESIMS data. This work was funded partially by the Australian Research Council, with additional support from PharmaMar (Madrid, Spain).

References

1 H. Zhang and R. J. Capon, *Org. Lett.*, 2008, **10**, 1959–1962.
2 K. Maynard and P. G. Parsons, *Cancer Res.*, 1986, **46**, 5009–5013.
3 C. X. Xu and P. G. Parsons, *Photochem. Photobiol.*, 1999, **69**, 611–616.
4 P. Skehan, R. Storeng, D. Scudiero, A. Monks, J. McMahon, D. Vistica, J. T. Warren, H. Bokesch, S. Kenney and M. R. Boyd, *J. Natl. Cancer Inst.*, 1990, **82**, 1107–1112.